

We are IntechOpen, the world's leading publisher of Open Access books Built by scientists, for scientists

5,900

Open access books available

145,000

International authors and editors

180M

Downloads

Our authors are among the

154

Countries delivered to

TOP 1%

most cited scientists

12.2%

Contributors from top 500 universities



WEB OF SCIENCE™

Selection of our books indexed in the Book Citation Index
in Web of Science™ Core Collection (BKCI)

Interested in publishing with us?
Contact book.department@intechopen.com

Numbers displayed above are based on latest data collected.
For more information visit www.intechopen.com



Modeling and Design of Flexure Hinge-Based Compliant Mechanisms

Sebastian Linß, Stefan Henning and Lena Zentner

Abstract

A compliant mechanism gains its mobility fully or partially from the compliance of its elastically deformable parts rather than from conventional joints. Due to many advantages, in particular the smooth and repeatable motion, monolithic mechanisms with notch flexure hinges are state of the art in numerous precision engineering applications with required positioning accuracies in the low micrometer range. However, the deformation and especially motion behavior are complex and depend on the notch geometry. This complicates both the accurate modeling and purposeful design. Therefore, the chapter provides a survey of different methods for the general and simplified modeling of the elasto-kinematic properties of flexure hinges and compliant mechanisms for four hinge contours. Based on nonlinear analytical calculations and FEM simulations, several guidelines like design graphs, design equations, design tools, or a geometric scaling approach are presented. The obtained results are analytically and simulatively verified and show a good correlation. Using the example of a path-generating mechanism, it will be demonstrated that the suggested angle-based method for synthesizing a compliant mechanism with individually shaped hinges can be used to design high-precise and large-stroke compliant mechanisms. The approaches can be used for the accelerated synthesis of planar and spatial flexure hinge-based compliant mechanisms.

Keywords: compliant mechanism, flexure hinge, deformation behavior, motion behavior, modeling, design

1. Introduction

A mechanism is generally understood as a constrained system of bodies designed to convert forces or motions. Fulfilling the function of power transmission (drive in the actuator system) or motion transmission (guidance in the positioning system), mechanisms are typical parts of a mechatronic motion system. For the realization of high-precise motion, increasingly compliant mechanisms are used instead of rigid-body mechanisms. A mechanism that gains its mobility fully or partially from the compliance of its elastically deformable parts rather than from rigid-body joints only is named as compliant mechanism [1, 2].

In precision engineering and micromechanics, there are increasingly high requirements for the motion system—especially regarding the smoothness, resolution, and repeatability of the motion. Therefore, compliant mechanisms with

concentrated or distributed compliance have become established for special positioning [3], adjustment [4], manipulation [5], or metrology [6] tasks. In these monolithic mechanisms, flexure hinges are mostly used as materially coherent revolute joints [7], while a high motion accuracy in the micrometer range can especially be achieved by common notch flexure hinges [8].

Nevertheless, the output stroke or motion range of such compliant mechanisms is considerably limited by the material strength since identical circular notch shapes are used for all hinges in the mechanism in most cases, even if they achieve different rotation angles. For high-strength metals, which are typically used for precision engineering applications, the rotation of flexure hinges is limited to small angles of a few degrees [9]. The demand for a larger angular deflection and a lower shift of the rotational axis results in numerous possible notch shapes and in a variety of sometimes very complex types of a separate flexure hinge, like the butterfly hinge [10]. Alternatively, mechanisms with a significantly increased hinge number in the kinematic chain are proposed to increase the range of motion, for example [11]. To further increase the stroke, often complex combinations of several substructure mechanisms are used in planar or spatial compliant stages, for example, reported in [9].

The sequential procedure including structural type synthesis, dimensional synthesis, and embodiment design, often used for rigid-body mechanisms, cannot be applied to compliant mechanisms straightforward, since the force/displacement limits of the flexure hinges must be matched with the required motion task. Thus, kinematic and kinetic behavior must be considered simultaneously for synthesis. Furthermore, the complex deformation and motion behavior of compliant mechanisms complicates both their accurate modeling and purposeful design. Hence, the synthesis is iterative, nonintuitive, and often time-consuming so far, and specific optimization approaches, for example [12], cannot be generalized. However, optimizing the shapes of easy-to-manufacture and mainly used notch flexure hinges may prove useful in the synthesis of compliant mechanisms. Among many possible notch shapes, power function flexure hinges, based on the higher order polynomial hinges suggested in [13], are especially suitable because they are highly variable and allow a simplified modeling, too [14].

In this chapter, a survey of different methods for the general and simplified modeling of the elasto-kinematic properties of flexure hinges and compliant mechanisms is provided for four certain hinge contours, the circular, the corner-filletted, the elliptical, and the power function-based contours, with different exponents. Based on nonlinear analytical calculations and FEM simulations, several approaches and guidelines like design graphs, design equations, design tools, or geometric scaling are presented which can be used for the flexure hinge design. The results are confirmed by means of analytical modeling and FEM simulation. The main approach with regard to the mechanism synthesis is to design each flexure hinge in a compliant mechanism individually in dependence of the known relative rotation angles in the rigid-body model. A four-bar path-generating mechanism is used as an example to show the benefits of the synthesis method regarding both a high precision and a large stroke in comparison to the use of identical notch geometries. Thus, the need for simulation is reduced.

2. Flexure hinge-based compliant mechanisms

A structural part of a compliant mechanism with a greatly increased compliance can be seen as a compliant joint, which allows at least one relative motion due to

deformation, but it is normally limited to a localized area. In dependence of the form of the relative motion, three types for a joint with one degree of freedom ($f = 1$) are existing, the revolute pair, the prismatic pair, and the screw pair (see **Table 1**).

Conversely to rigid-body joints, in which two rigid links form either a form-closed or force-closed pairing, neighboring links of a compliant mechanism are connected to each other in a materially coherent way. Thus, an increased compliance can be achieved through a variation of geometry and/or a variation in material, while the geometric design is in the focus of the following investigations. In this chapter, macroscopic compliant mechanisms with flexure hinges realizing a desired rotary motion are regarded, since they are used in most cases.

2.1 Analysis and synthesis of compliant mechanisms

For the synthesis of a compliant mechanism, three main approaches are suggested in literature: synthesis through the rigid-body replacement method (e.g., [15]), synthesis through the topology optimization method (e.g., [16]), and synthesis through constrained-based methods (e.g., [17]). In order to realize a better guidance accuracy, the rigid-body replacement synthesis is more suitable than the topology optimization synthesis [18]. Therefore, here the purposeful design of a compliant mechanism based on the rigid-body model is meant by speaking of synthesis. The geometric design of the incorporated flexure hinges is a key point during the synthesis, because often multi-objective design criteria exist.

Regarding a four-bar Roberts mechanism realizing an approximated straight-line path of a coupler point P , the rigid-body mechanism and the compliant counterpart are shown in **Figure 1**. For the replacement, the same initial position of the compliant mechanism with the crank angle γ is used as in the rigid-body model. The Roberts mechanism with four hinges is a typical path-generating mechanism which is used for the rectilinear guidance of a coupler point in precision engineering applications, for example [19–22].

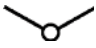
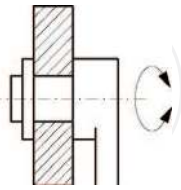
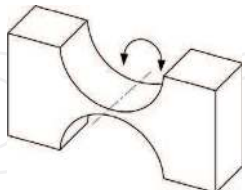

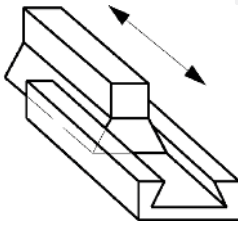
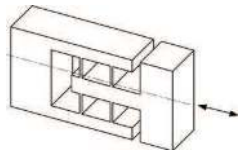
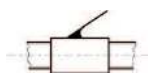
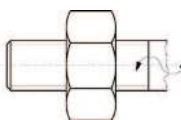
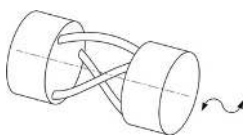
Joint type	Symbol	Rigid-body joint	Compliant joint
Revolute pair (hinge)			
Prismatic pair			
Screw pair			

Table 1.
 Classification of joints with $f = 1$ by means of the form of relative motion.

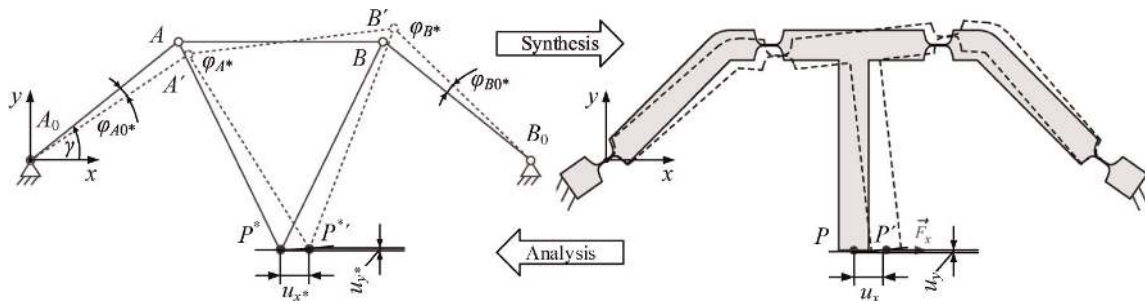


Figure 1.

Analysis and synthesis of a compliant mechanism based on the rigid-body model using the example of a path-generating Roberts mechanism.

In contrast to the synthesis, the analysis describes the modeling of the rotation axes and link lengths of the rigid-body model based on the compliant mechanism, for example [1, 2]. Additionally, the bending stiffness of all hinges has to be considered.

With a few exceptions (e.g., [5, 23]), almost identical flexure hinges are used in the same single compliant mechanism. However, the relative rigid-body-based rotation angles φ^* for the desired motion of the mechanism are different for the incorporated hinges in most cases. Due to the different rotation angles, different flexure hinge contours are also required. Because the deflection angle φ of each flexure hinge is approximately equal to φ^* [24], an angle-based and goal-oriented four-step synthesis method for using individually shaped notch flexure hinges in one compliant mechanism can be applied [25]. The basic phases are (cf. Section 4):

- i. Synthesis of a suitable rigid-body model
- ii. Replacement and design of the compliant mechanism
- iii. Goal-oriented and angle-based geometric design of the flexure hinges
- iv. Verification of results and proof of requirements.

In literature, the specific geometric design of the flexure hinges during synthesis is only considered when using almost identical hinges in a compliant mechanism and standard contours with a limited variability like corner-filletted hinges [26].

2.2 Classification of compliant mechanisms

In dependence of the existence of rigid-body joints, compliant mechanisms can be separated into the categories of fully compliant mechanisms or partially compliant mechanisms, while the presented design guidelines in this chapter are suitable for both. Additionally, fully and partially compliant mechanisms can be separated into mechanisms with concentrated or distributed compliance [2] (see **Table 2**), while mechanisms with concentrated compliance are regarded here.

Furthermore, the presented results in this chapter are focused on planar compliant mechanisms (see **Figure 2**). Nevertheless, the suggested methods and design approaches can be used for spherical and spatial compliant mechanisms, too.

2.3 Classification of flexure hinges

A flexure hinge is understood as a compliant joint which approximately acts as a hinge due to flexural bending. Thus, the form of relative motion can only be idealized as a rotation. Because of their monolithic arrangement, compliant joints

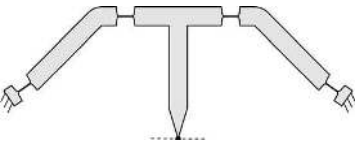
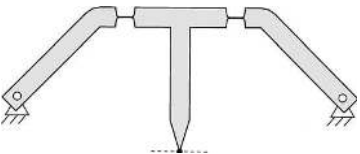
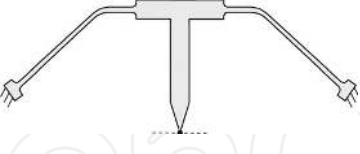
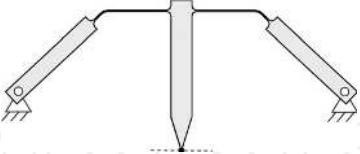
Mechanism	Fully compliant mechanism	Partially compliant mechanism
With concentrated compliance		
With distributed compliance		

Table 2.
 Classification of compliant mechanisms by means of the structural design and the distribution of compliance.

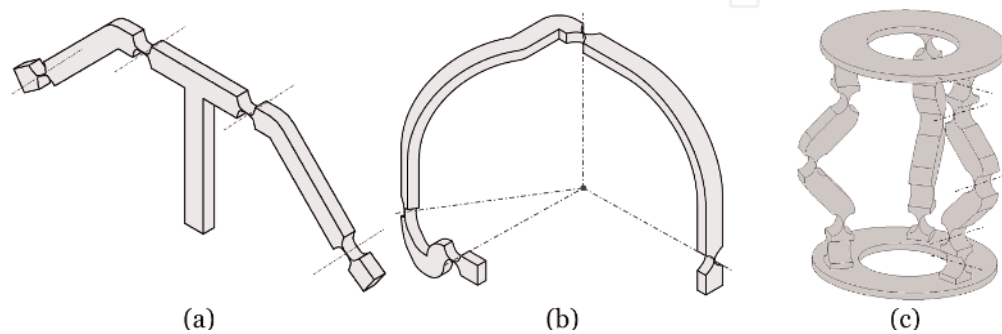


Figure 2.
 Classification of compliant mechanisms by means of the position of the revolute axes: (a) planar mechanism, (b) spherical mechanism, and (c) spatial mechanism according to [27].

provide numerous approaches for the design of a flexure hinge. Based on the well-described leaf-type flexure hinge [28], many different flexure hinge types have been developed in the past decades or introduced in recent works in order to realize a larger angular deflection and/or a more precise rotation (see **Figure 3**) [10, 29–31]. Many more flexure hinge types are classified in [32].

The design guidelines in this chapter are focused on notch flexure hinges because different design goals can be met by selecting between comparable, simple notch hinge designs already, largely due to a great contour variety [32]. Due to their low complexity, they are easy to manufacture and therefore mainly used in compliant mechanisms, especially in kinematic chains with a higher link number.

Notch flexure hinges have often geometrically been designed so that various cutout geometries are proposed to describe the variable contour height. There are mostly predefined basic geometries which lead to the typical precise hinge with a semicircular contour, the large-deflective hinge with a corner-filletted contour, or the elliptical hinge as a compromise [33]. Furthermore, flexure hinges are designed with other elementary or complex geometries (e.g., [34]) to realize special properties. Higher order polynomial functions are not state of the art. But among the

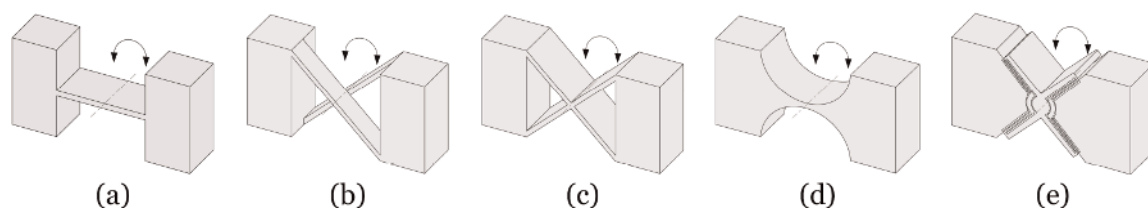
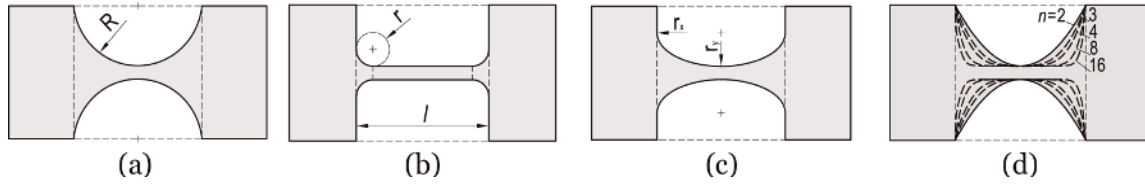


Figure 3.
 Typical types of flexure hinges used to achieve a rotational motion with one degree of freedom ($f = 1$): (a) leaf-type hinge, (b) crossed leaf-type hinge, (c) prismatic crossed hinge, (d) notch hinge, and (e) multi-trapezoidal hinge/butterfly hinge.


Figure 4.

Typical geometries of notch flexure hinges with their contour-specific parameters: (a) circular contour with radius R , (b) corner-filletted contour with stress-optimal fillet radius $r = 0.1 l$, (c) elliptical contour with major axis r_x and minor axis r_y , and (d) variable power function-based contour, shown for different exponents n .

variety of geometries, especially these contours offer high optimization potential, while a comparatively simple modeling is possible [35]. Thus, the advantages of the polynomial contour are implemented and extended to a power function contour to offer a wider range of possible hinges due to a rational exponent n [14], with

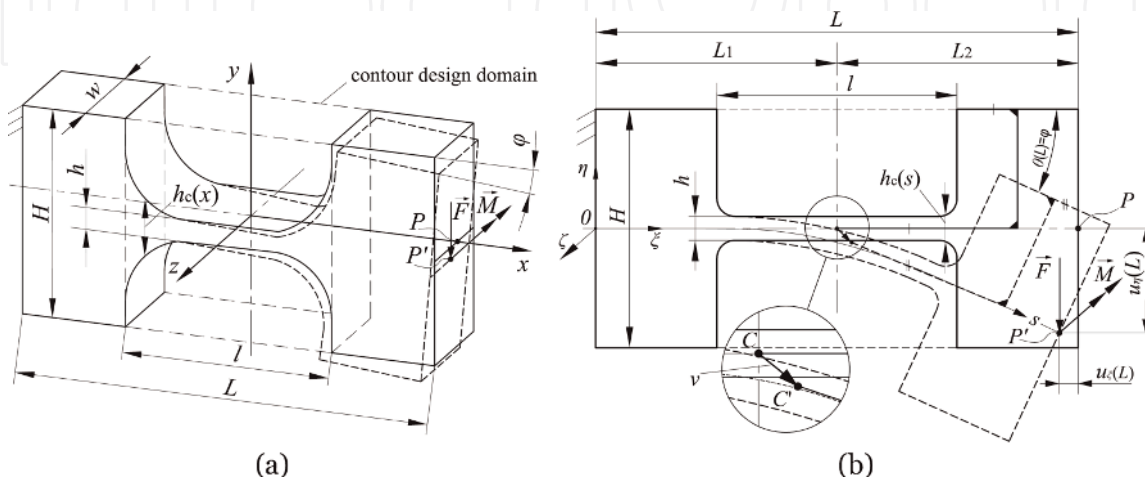
$$h_c(x) = h + \frac{(H - h)}{\left(\frac{l}{2}\right)^n} |x|^n, \text{ with } n \in \mathbb{R}. \quad (1)$$

In the following, four certain flexure hinge contours are considered (see **Figure 4**): the semicircular contour, the corner-filletted contour with a stress-optimal and hinge length-related fillet radius $r = 0.1 l$ [36], the semielliptical contour, and the power function-based contour. The remaining contour height functions and detailed information about the depicted segment-wise contour modeling are given in [14]. Many more notch geometries are classified in [32].

3. Modeling and design of notch flexure hinges

As a flexure hinge, a monolithic, small-length, and elastically deformable segment of a compliant mechanism with the variable and symmetric contour height $h_c(x)$ and a rectangular cross section is defined, which provides a relative rotation of two adjacent links mainly limited due to bending stress (see **Figure 5**). Since not only the notch segment undergoes deformation, it is recommended to model the hinge with little segments of both adjacent links and as a 3D solid structure [37, 38].

In the following, three important rotational performance properties are considered. A flexure hinge provides a restoring force (a property called *bending stiffness*), which may be beneficial in precision applications, too. Depending on the material


Figure 5.

Modeling of a notch flexure hinge under a bending moment and/or a transverse force load: (a) hinge with a variable hinge height within the contour design domain, the geometric parameters and the deflected state and (b) parameters for the theoretical characterization and approach for the definition of the rotational axis shift based on guiding the center with a constant distance, the fixed center approach.

coherence, the angular rotation of a flexure hinge is restricted by maximum acceptable stresses or elastic strains (*maximum angular deflection*). Therefore, the stroke of a compliant mechanism is limited as well through the joint with the largest deflection angle in the kinematic chain, assuming the same contours are used. In addition, no exact relative rotation is possible with a flexure hinge, because its axis of rotation is always shifted as geometric and load parameters vary (*rotational precision*) [36, 39]. In turn, this can lead to path deviations in the compliant mechanism compared with the rigid-body model that can no longer be considered negligible, especially in precision engineering applications [24, 40].

Regarding the influence on the flexure hinge properties, two main groups of geometric design parameters are existing, the hinge dimensions (L, l, H, h, w) and the hinge contour or notch shape (function $h_c(x)$), while the total height H represents the link height in the compliant mechanism, too. Hence, four geometric parameters—the hinge total length L , the hinge notch length l , the minimum hinge height h , and the hinge width w —can be varied within the design domain according to the following introduced dimensionless ratios:

$$\beta_L = \frac{L}{H}, \beta_l = \frac{l}{H}, \beta_h = \frac{h}{H}, \text{ and } \beta_w = \frac{w}{H}. \quad (2)$$

For a separate flexure hinge, it is known that the properties depend on the basic geometric dimensions as follows [41, 42]: the bending stiffness and maximum stress increase in particular as the minimum hinge height h increases and the rotational precision decreases with an increasing minimum height h . Furthermore, several different and partly contrary recommendations for some hinge dimension ratios of circular and corner-filletted flexure hinges are existing (cf. [32]).

Other than that, the high-strength aluminum alloy AW 7075 with Young's modulus $E = 72$ GPa, Poisson's ratio $\nu = 0.33$, and the admissible elastic strain limit $\varepsilon_{\text{adm}} = 0.5\%$ is chosen as a typical material which has been used for multiple high-precision engineering applications, for example [3, 21].

3.1 Nonlinear FEM simulation

For the quasi-static structural FEM simulation, performed with ANSYS Workbench 18.2, the hinge is modeled as a 3D structure with Solid186 hexahedral elements. The CAD model and FEM model are shown in **Figure 6**. The FEM model is considered with a fixed support on one side, and it is free on the opposite side. The free end is stepwise loaded with a bending moment or a directionally constant transverse force applied at an edge parallel to z . The analysis of two points on the loaded hinge side enables an accurate calculation of the rotation angle φ . Hence, the

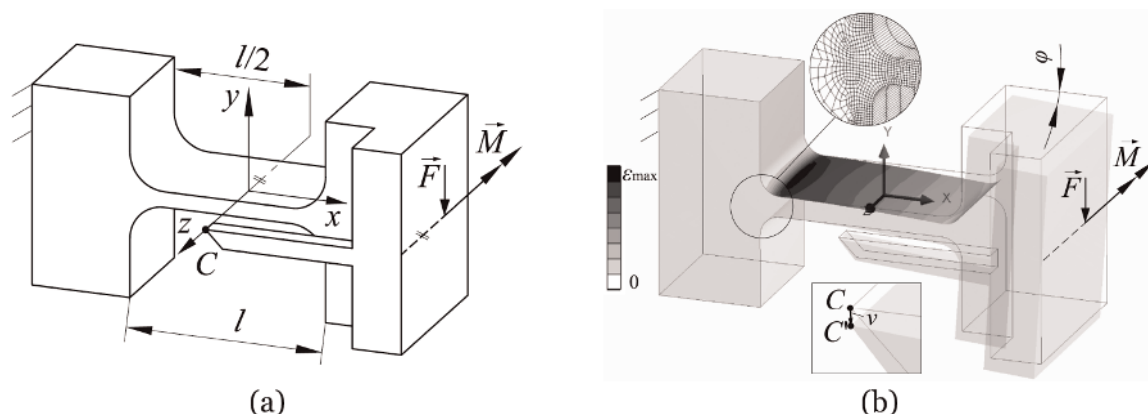


Figure 6. FEM-based characterization of a flexure hinge: (a) CAD model and (b) FEM model with deformed hinge and mesh details.

characteristic $M(\varphi)$ and $F(\varphi)$ curves can be determined. The maximum deflection angle φ_{\max} can be calculated in dependence of the regarded maximum value of the equivalent von Mises strain ε_{\max} . Moreover, large deflections are considered for an accurate comparison with the analytical calculations due to the nonlinear beam theory. Other assumptions are a linear material behavior and a comparable and fine discretization of the hinge, especially in areas of the minimum hinge height.

For the determination of the rotational precision, an additional part is added onto the CAD model according to the often used and chosen fixed center approach [36]. Based on guiding the center point C with a constant length $l/2$, the distance between C and C' defines the rotational axis shift v .

3.2 Design graphs

Among the four investigated flexure hinge contours (cf. **Figure 4**), the power function contour allows the modeling of a wide spectrum of different notch hinges. Depending on the exponent n and the hinge dimensions, arbitrary complex curves can be realized, or nearly any elementary geometry can be approximated. For a given deflection angle φ , it has been shown that 16th-order polynomial contours lead to low stress or strain values comparable to those of corner-filletted contours [13]. Furthermore, it was found that fourth-order polynomial contours allow for both a precise rotation and large rotation angles in general [24]. In addition, it is quite possible to realize required hinge properties by arbitrarily varying n .

Based on a geometrically nonlinear FEM simulation using a given displacement at the free end, design graphs for power function-shaped flexure hinges with typical dimension have been created (see **Figure 7**) (cf. [24]). Thus, the bending moment M can be easily determined depending on the rotation angle φ and n . Analogously, the transverse force F results in good approximation by considering the moment M divided by the half-length $L/2$ (cf. **Table 4**) [33]. Furthermore, a minimum required exponent n can be read out depending on φ and the admissible material strain ε_{adm} . The determination of n is also possible with an odd or rational number.

3.3 Nonlinear analytical calculation

As long as the dimensions of the cross section are small compared to the rod length, the nonlinear theory for large deflections of curved rodlike structures is sufficient to describe the deformation behavior of compliant systems [2]. Hence, the analytical investigations are based on the well-known Euler-Bernoulli's theorem for a static problem of a slender structure with an assumed axial inextensible line. The additional assumption is made that Saint-Venant's principle and Hooke's law apply. If a flexure hinge is modeled together with adjacent deformable link segments as a bent rod with a variable height, this theory is assumed to be suitable, too. Further specific effects relevant for notch flexure hinges have to be expected especially for very thin hinges [43], but they are neglected here with regard to general design guidelines. Among them are shear deformation [44], stress concentration [45], anticlastic bending [46], or manufacturing imperfections [47].

For the analytical calculation, a stationary coordinate system $\{\xi, \eta, \zeta\}$ is considered with the origin 0 at the fixed end (cf. **Figure 5b**). The arc length s is used to characterize the neutral axis in the deflected state. The bent hinge undergoes a displacement $u_\xi(s)$ and $u_\eta(s)$ for each coordinate along s , which lead to the deflection angle $\theta(s)$. The curvature $\kappa(s)$ is the gradient of $\theta(s)$. Hence, four nonlinear differential equations are used to model a flexure hinge in the deflected state:

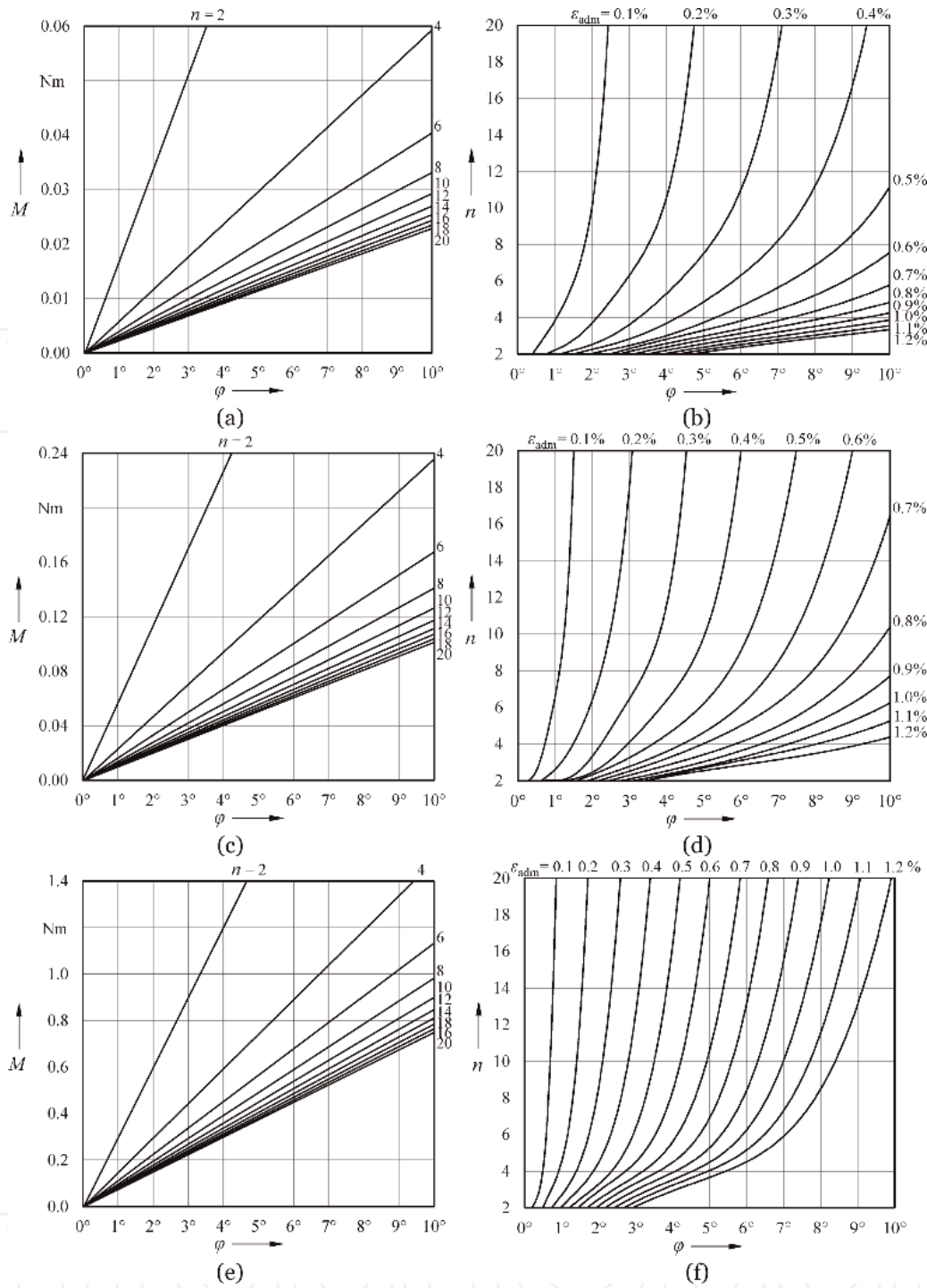


Figure 7. FEM-based design graphs to determine the bending moment M (depending on the rotation angle φ and the exponent n of each power function flexure hinge) or to determine the minimum exponent n (depending on φ and the admissible material strain ϵ_{adm}), created for different hinge heights and $\beta_L = 3$, $\beta_1 = 1$, $\beta_w = 0.6$ (cf. [24]): (a) M for $\beta_h = 0.03$, (b) n for $\beta_h = 0.03$, (c) M for $\beta_h = 0.05$, (d) n for $\beta_h = 0.05$, (e) M for $\beta_h = 0.1$, and (f) n for $\beta_h = 0.1$.

$$\frac{dM_\zeta}{ds} + F \cos \theta = 0, \quad (3)$$

$$\frac{d\theta}{ds} - \kappa = 0, \text{ with } \kappa = \frac{M_\zeta}{E I_\zeta}, \quad (4)$$

$$\frac{du_\xi}{ds} - \cos \theta + 1 = 0, \quad (5)$$

$$\frac{du_\eta}{ds} - \sin \theta = 0. \quad (6)$$

The initial curvature is zero here, because a fully symmetric flexure hinge is considered. A numerical solution is done for the system of differential equations with the subsequent boundary conditions for a bending moment at the loaded side:

$$M_\zeta(L) = M, \theta(0) = 0, u_\xi(0) = 0, u_\eta(0) = 0, \quad (7)$$

and with the following conditions for a transverse force load.

$$M_\zeta(L) = 0, \theta(0) = 0, u_\xi(0) = 0, u_\eta(0) = 0. \quad (8)$$

The boundary value problem is solved numerically with MATLAB [14]. At the end of this procedure, all four parameters κ , θ , u_ξ , and u_η are obtained for each point s along the deformed neutral axis, and further results for the considered hinge properties can be estimated. The bending stress σ is analyzed after linear beam theory to characterize the maximum stress of the entire flexure hinge for a given deflection angle. According to Hooke's law, stress and strain are linearly dependent on each other by E , wherefore the bending strain ε is considered. The maximum absolute value of the strain always occurs at the outer fiber for the maximum η -coordinate, which corresponds with the contour height function of the hinge. In addition, the absolute value of the rotational axis shift v , based on the fixed center approach, is put together from the axis shift of point C in ξ and η -direction [14].

3.4 Design equations

To provide closed-form equations which can be used for the simplified flexure hinge synthesis regarding all three rotational properties, six design equations have been developed for both load cases based on the analytical characterization due to the described nonlinear theory (see **Table 3**). SI units must be used for all parameters. The load acts close to the hinge center at $L = 2H$ in this case, while only the elastic properties are almost independent from the value of this distance for the bending moment load [33]. The equations are accurately valid for a rotation angle up to $\varphi = 5^\circ$. The calculation of results for larger angles is nevertheless possible.

With regard to an accelerated and unified synthesis of compliant mechanisms, the general design equations are concise and thus advantageous. With only two coefficients, their structural form is simple, contour-independent, and, with respect to the maximum hinge height or link height H as scaling factor, dimensionless.

The further necessary contour-specific coefficients of all six design equations are given in **Table 4** for the four regarded hinge contours and an appropriate parameter range of the hinge dimensions, the hinge length ratio β_l ($0.5 \leq \beta_l \leq 1.5$) and the hinge height ratio β_h ($0.03 \leq \beta_h \leq 0.1$). The coefficients of the used power functions are determined with MATLAB based on a fitting procedure in order to attain the smallest maximum error over all calculated result points [33].

Property	Bending moment	Transverse force
Bending stiffness	$\frac{M}{\varphi} = k_{M1} E \beta_w \beta_l^{(-k_{M2})} \beta_h^{(2+k_{M2})} H^3$ (9)	$\frac{F}{\varphi} = k_{F1} E \beta_w \beta_l^{(-k_{F2})} \beta_h^{(2+k_{F2})} H^2$ (10)
Maximum angular deflection	$ \varphi_{\max} = \frac{\varepsilon_{\text{adm}}}{6 k_{M1}} \left(\frac{\beta_l}{\beta_h}\right)^{k_{M2}}$ (11)	$ \varphi_{\max} = \frac{\varepsilon_{\text{adm}}}{12 (1-k_{\text{crit}})^{k_{F1}}} \left(\frac{\beta_l}{\beta_h}\right)^{k_{F2}}$ (12)
Rotational precision/axis shift	$\frac{v}{\varphi^2} = k_{vM1} \beta_l^{k_{vM2}} \beta_h^{(1-k_{vM2})} H$ (13)	$\frac{v}{\varphi} = k_{vF1} \beta_l^{k_{vF2}} \beta_h^{(2-k_{vF2})} H$ (14)

Table 3.
Contour-independent closed-form design equations based on analytical modeling.

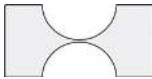
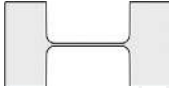


Hinge contour	k_{M1} [10^{-3}]	k_{M2}	k_{F1} [10^{-2}]	k_{F2}	k_{crit}	k_{dM1} [10^{-3}]	k_{dM2}	k_{dF1} [10^{-2}]	k_{dF2}
Circular 	107.90	0.52	10.55	0.51	0.5	99.85	0.52	19.12	0.94
Corner-filleted 	83.95	0.96	8.41	0.96	$0.5-0.2\beta_l$	85.76	0.95	9.20	1.89
Elliptical 	82.50	0.54	8.27	0.54	0.5	114.35	0.57	18.21	1.14
Power function (fourth order) 	112.07	0.74	11.22	0.74	$0.4\beta_l^{(-0.081)}$ $\beta_h^{(-0.048)}$	71.32	0.73	6.24	1.47

Table 4.
 Load and contour-specific coefficients for the design equations in Table 3.

The relative discrepancy errors between the design equation results and the analytical results, a comparison with FEM results, as well as coefficients for further power function contours are mentioned in [48]. According to the theory, the accuracy of the results is nearly independent of the parameter range for the hinge width β_w . The maximum strain occurs contour-independently in the hinge center for a bending moment. An additional factor k_{crit} has become necessary to consider the deviation of the critical strain location from the center for a transverse force load, especially for corner-filleted and power function hinges (cf. Section 3.7).

3.5 Design tool detasFLEX

Moreover, computational design tools may prove useful for the comprehensive analysis and synthesis of various notch flexure hinges, such as the developed tool detasFLEX [14], which is also based on the described nonlinear modeling approach (cf. Section 3.3). The graphical user interface (GUI) is shown in Figure 8.

The design tool was created with MATLAB as a stand-alone software application which only requires the license-free runtime environment. Four flexure hinge contours are considered, the circular, corner-filleted, elliptical, and power function-based contours (cf. Figure 4). Various geometric and material parameters may be realized to allow for a broad usability in different cases. The calculation is possible for a bending moment and a transverse force as well as both loads combined for different lengths of each hinge side. The computation of results is further possible for all three load cases with a given load or a given rotation angle up to 45° . A wide range of result parameters may be computed, and the most important hinge performance properties like the deformed neutral axis, the bending stiffness, the rotational precision, and the elastic strain distribution are illustrated in the form of diagrams. Additionally, a preview of the exact hinge geometry with the instant visualization of input changes is implemented. Also, values for the angle or load, axis shift, strain distribution, maximum strain, and maximum possible rotation angle are calculated. Using a corner-filleted hinge, for example, the deviation of the bending stiffness between the FEM and design tool results is in the range of 0.1–9.4% for a given rotation angle of 10° [14].

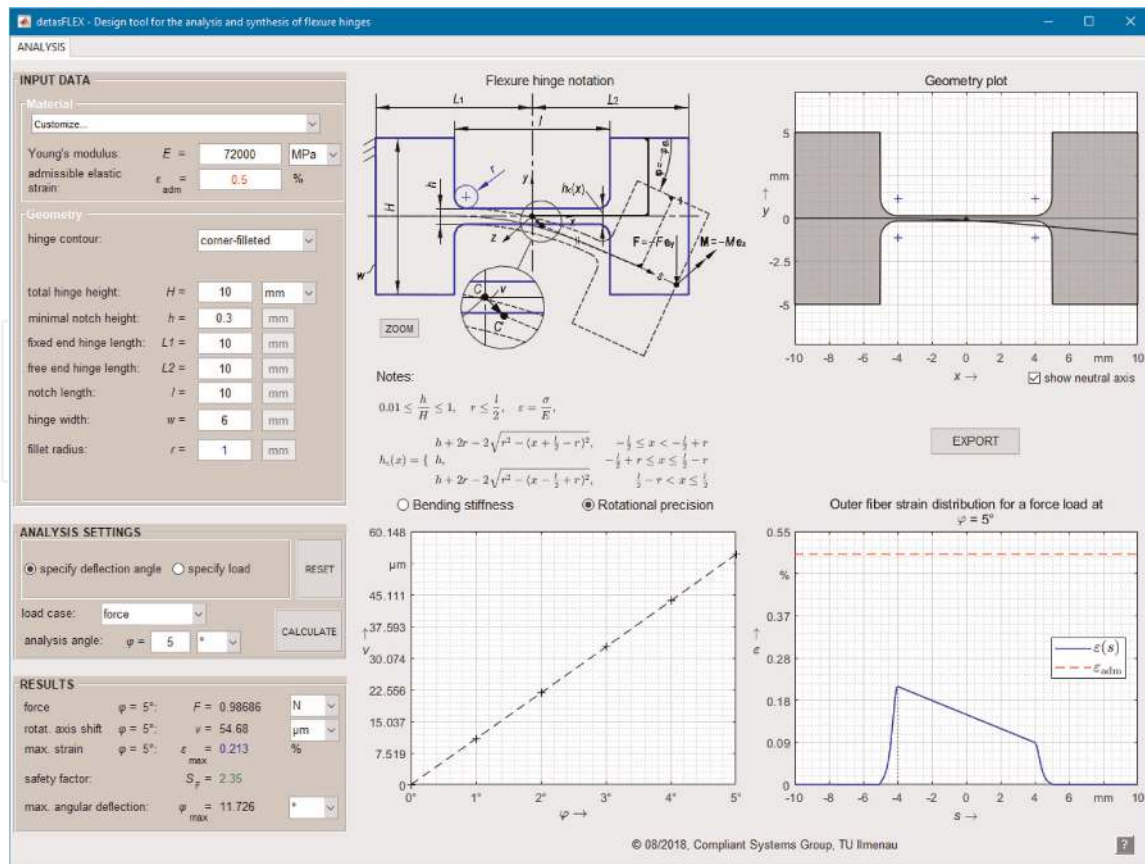


Figure 8. Graphical user interface of the computational design tool *detasFLEX*, shown using the example of a corner-*filleted flexure hinge*.

DetasFLEX enables a wide variety of different geometry, material and contour selections, as well as multiple analysis criteria and settings so that numerous notch flexure hinges for diverse tasks may be accurately analyzed within a few seconds. Thus, each hinge in a compliant mechanism can be designed purposefully and individually. Based on this, the PC-based synthesis is generally possible, too.

3.6 Comparison of results and usability

The different methods for modeling the elasto-kinematic flexure hinge properties described above are compared in **Table 5** using the example of a power function-shaped hinge of the fourth order. The design tool results and analytical modeling are mentioned together due to the equality of the values. It is obvious that

Method	Bending moment				Transverse force			
	$\varphi = 5^\circ$	$\epsilon_{adm} = 0.5\%$			$\varphi = 5^\circ$	$\epsilon_{adm} = 0.5\%$		
	M [Nm]	v [μm]	ϵ_{max} [%]	φ_{max} [$^\circ$]	F [N]	v [μm]	ϵ_{max} [%]	φ_{max} [$^\circ$]
FEM	0.0294	2.190	0.414	6.039	2.946	9.980	0.439	5.695
Design graph	0.029	—	0.43	5.3	2.9	—	0.43	5.3
Design equation	0.0284	2.107	0.438	5.707	2.842	8.490	0.459	5.403
Design tool/ analytic	0.0277	2.226	0.428	5.839	2.785	9.459	0.450	5.562

Table 5. Comparison of results for the method-dependent elasto-kinematic properties using the example of a power function hinge of the fourth order ($\beta_L = 2$, $\beta_1 = 1$, $\beta_h = 0.03$, $\beta_w = 0.6$).

the suggested design guidelines and tools allow the accurate and simplified determination or calculation of the deformation, stress/strain, and motion behavior with respect to the assumptions and geometric restrictions.

Regarding the usability, the design tool provides the most comprehensive support for the modeling and design of various notch flexure hinges (see **Table 6**).

Additionally, the design equations are also easy to use for the four regarded hinge contours. Furthermore, it becomes obvious that the determination method influences the possible values for the hinge dimensions and the power function exponent n as well as valid ranges of the deflection angle. Due to compactness, in Section 4.3, n is exemplarily determined based on the design graph approach.

In conclusion, all three design aids can be used for the accelerated contour-specific quasi-static analysis of the elasto-kinematic properties of notch flexure hinges with no need for further iterative and time-consuming simulations. Moreover, the guidelines and tools may be used for the systematic angle-dependent synthesis of compliant mechanisms with differently optimized flexure hinges (cf. Section 4).

3.7 Influence of the contour on the elasto-kinematic hinge properties

Independent of the selected method, the influence of the flexure hinge contour on the elasto-kinematic hinge properties can be generalized, especially for thin hinges. In **Figure 9**, the analytical results are exemplarily presented for a force load.

The load-angle behavior is almost linear for the regarded angular deflection up to 5° . The following order can be concluded from the lowest to the highest stiffness: the corner-filleted, power function, elliptical, and circular contour (**Figure 9a**).

Because the maximum strain value limits the deflection, the maximum rotation angle of a flexure hinge is always possible with a corner-filleted contour, while a circular contour leads to the lowest possible angles (**Figure 9c**). Furthermore, the asymmetric strain distribution due to the transverse force load is obvious, especially for a corner-filleted contour (**Figure 9d**). Due to the notch effect, the strain is concentrated in the hinge center for a circular and elliptical contour, while the other contours lead to a more even strain distribution along the hinge length.

Furthermore, the hinge contour has a strong influence on the axis shift, which can be in the range of some micrometers up to submillimeters in dependence of β_l and especially β_h . With regard to a high rotational precision or a small axis shift, the following order is existing for thin hinges: the circular contour, elliptical contour or power function contour to the same extend, and corner-filleted contour (**Figure 9b**).

Thus, the power function contour of the fourth order simultaneously provides a large angular deflection and a high rotational precision. The influence of the basic hinge dimensions is further investigated in [33]. An influence of β_L is to be expected, too.

4. Modeling and design of compliant mechanisms

In this section, the synthesis method presented in Section 2.1 is applied to a path-generating mechanism to explore the angle-based approach of the optimal design with individually shaped flexure hinges in one single compliant mechanism using power functions. Therefore, a symmetric four-bar Roberts mechanism with four hinges, realizing the guidance of the coupler point P on an approximated rectilinear path (cf. [19–22]), is investigated. The rigid-body model and the compliant mechanism are shown in **Figure 1** in the initial and deflected positions.

Method, related reference	Hinge contours			Power function	Domain and value of n	Hinge dimensions $\beta_L, \beta_b, \beta_h$, and β_w	Range of φ	Result criteria	Modeling effort/ computation time
	Circular	Corner-filleted	Elliptical						
FEM, nonlinear, e.g., [24]	x	x	x	x	Arbitrary	Arbitrary	Arbitrary	Arbitrary	Great/ high
Analytical, nonlinear, e.g., [2]	x	x	x	x	Arbitrary	Arbitrary	Arbitrary	Arbitrary	Great/ low
Design graph [24]				x	$2 \leq n \leq 20$	Predefined (three cases for β_h)	$\leq 10^\circ$	$M(\varphi), (F(\varphi)), \varphi_{\max}, \varepsilon_{\max}$	None
Design Eq. [33, 48]	x	x	x	x	2, 3, 4, 8, 16	Constrained	$\leq 5^\circ$	$M(\varphi), F(\varphi), v(\varphi), \varphi_{\max}, \varepsilon_{\max}$	None
Design tool [14]	x	x	x	x	$1.1 \leq n \leq 50$	Slightly constrained	$\leq 45^\circ$	$M(\varphi), F(\varphi), v(\varphi), \varphi_{\max}, \varepsilon_{\max}, \varepsilon(s)$	Little/low

Table 6. Comparison of usability of the presented methods, guidelines, and approaches for the modeling and design of notch flexure hinges.

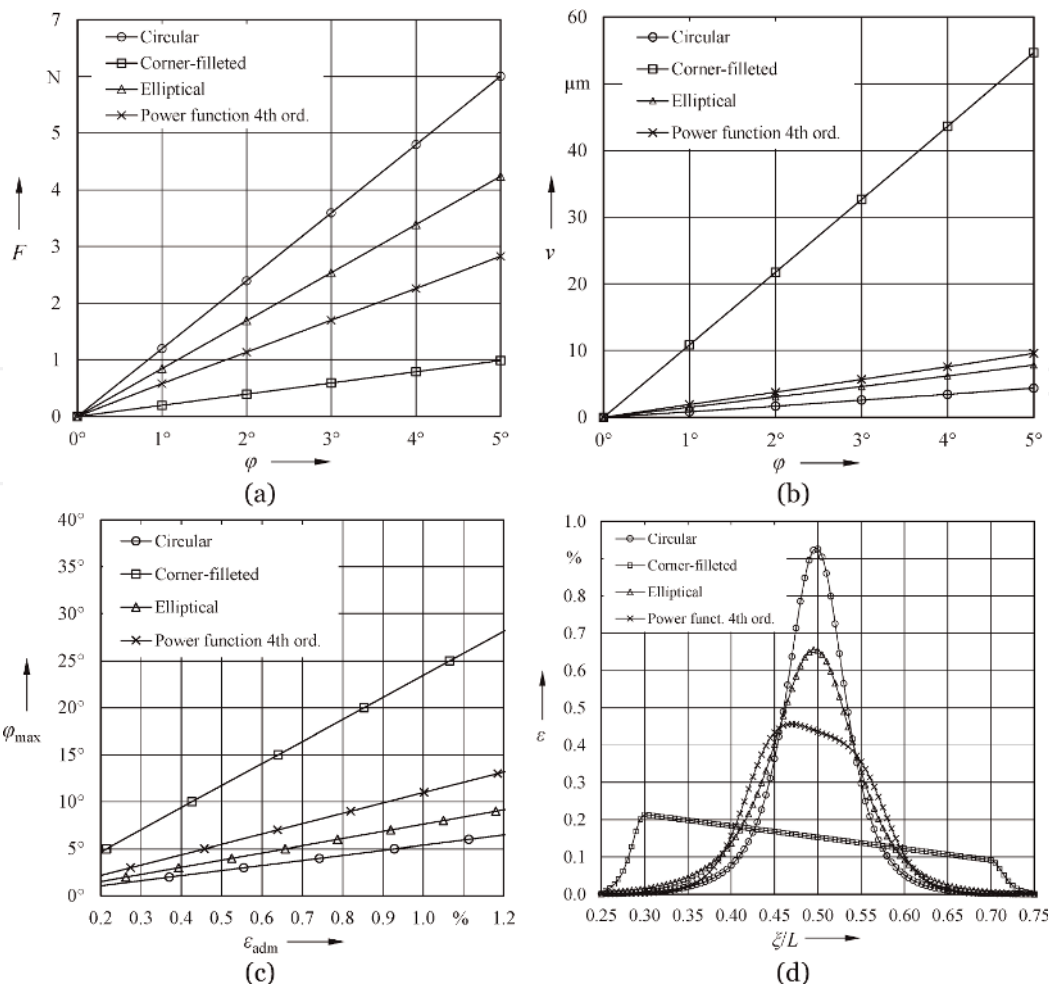


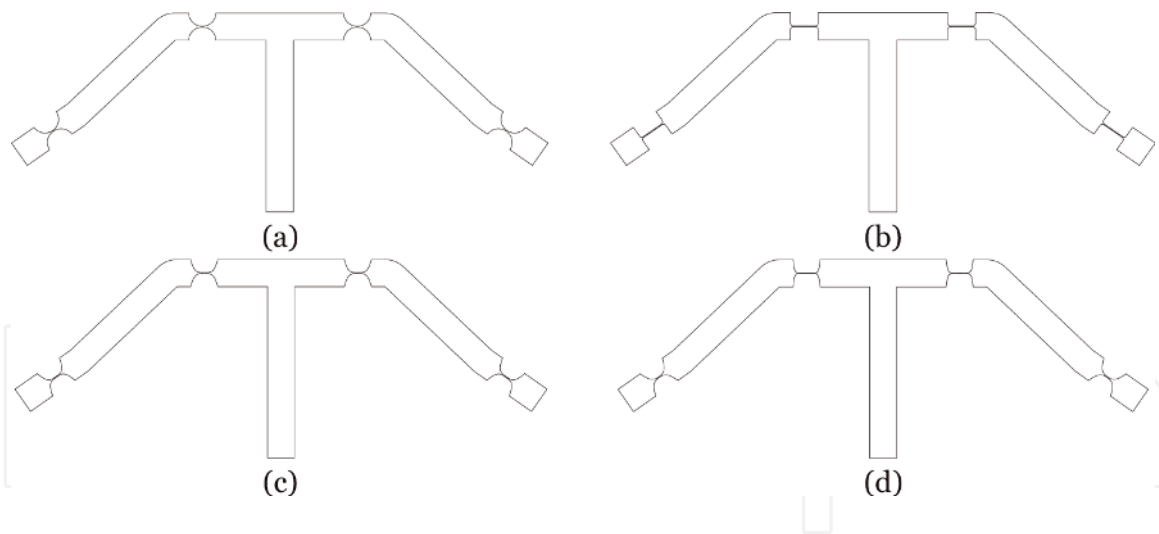
Figure 9. Analytical results for the influence of the flexure hinge contour on the hinge properties ($\beta_L = 2$, $\beta_1 = 1$, $\beta_h = 0.03$, $\beta_w = 0.6$, force load): (a) bending stiffness, (b) axis shift, (c) maximum angular deflection, and (d) outer fiber strain distribution for $\varphi = 5^\circ$.

The link lengths are suitably chosen as $\overline{A_0A} = \overline{B_0B} = 66.6$ mm, $\overline{AB} = 56.6$ mm, $\overline{A_0B_0} = 165.71$ mm, and $\overline{AP} = \overline{BP} = 73.6$ mm, according to [24]. Furthermore, the mechanism position with the replacement angle $\gamma = 35^\circ$ is used. Thus, applying the input displacement $s = u_{xP}^* = u_{xP} = 10$ mm in point P , the relevant straight-line deviation for the rigid-body model results as $u_{yP}^* = -24.7$ μm .

4.1 Synthesis method based on individually shaped flexure hinges

A compliant mechanism with individually shaped power function flexure hinges is synthesized according to the synthesis method based on the relative rotation angles in the rigid-body model (cf. Section 2.1) exemplarily using the design graph approach (cf. Section 3.2). The resulting compliant mechanism is shown in **Figure 10d**. Furthermore, the mechanism properties are compared with three compliant mechanisms using identical hinges designed with circular, corner-filletted, or power function contours of the fourth order (see **Figure 10a–c**).

Following the rigid-body replacement approach, the flexure hinge centers are designed identical to the revolute joints. Next, suitable flexure hinge orientations are chosen with respect to the link orientations of the crank and the coupler (cf. Section 4.3). The main link parameters are specified as $H = 10$ mm and $\beta_w = 0.6$, while the same aluminum material as in Section 3 is used ($E = 72$ GPa, $\varepsilon_{\text{adm}} = 0.5\%$). Furthermore, comparable short and thin hinges are used with the hinge length ratio $\beta_l = 1$ and the height ratio $\beta_h = 0.03$ because they are especially suitable [24].


Figure 10.

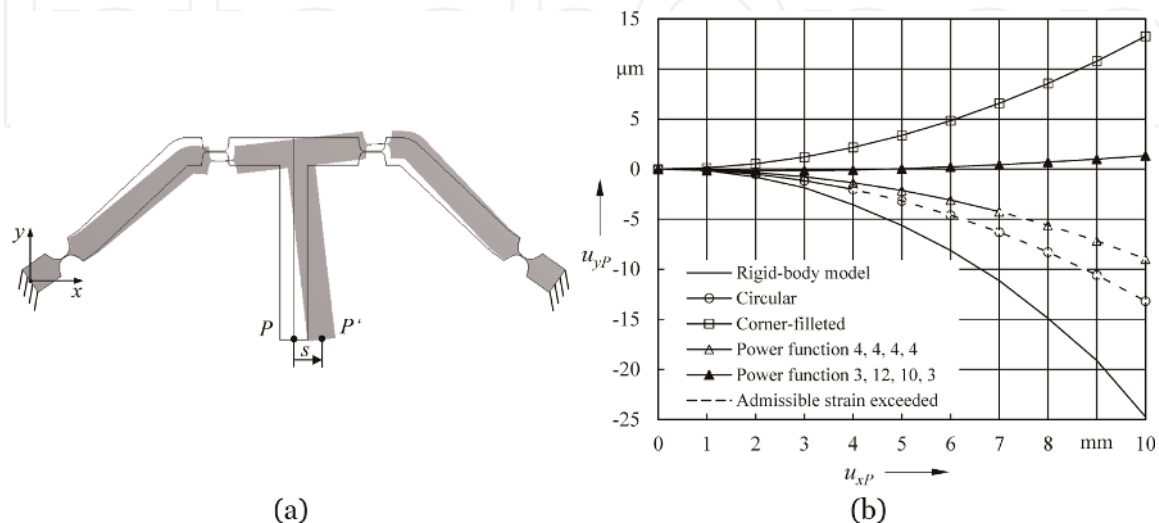
Designs of the compliant Roberts mechanism ($\beta_1 = 1$, $\beta_h = 0.03$) with (a) circular hinges ($R = H/2$), (b) corner-filleted hinges ($r = 0.1 l$), (c) identical power function hinges ($n = 4$), and (d) different power function hinges ($n_{A0} = 3$, $n_A = 12$, $n_B = 10$, $n_{B0} = 3$).

Based on the relative rigid-body-based rotation angles $\varphi_{A0}^* = 3.8^\circ$, $\varphi_A^* = 10.4^\circ$, $\varphi_B^* = 9.5^\circ$, and $\varphi_{B0}^* = 3.0^\circ$, which result through a simple kinematic analysis, the power function exponents can be determined for the assumption $\varphi = \varphi^*$. According to the designed graph in **Figure 7b**, the exponents result in $n_{A0} = 3$, $n_A = 12$, $n_B = 10$, and $n_{B0} = 3$. The exponents are exemplarily determined as even numbers, while rational exponents are also possible for a more specific design.

4.2 Nonlinear FEM simulation

For the quasi-static structural and geometrically nonlinear FEM simulation of the compliant Roberts mechanisms, the same settings as for a separate hinge are used (cf. Section 3.1). The results for the motion path of the coupler point P are shown in **Figure 11** for a given x -displacement in dependence of the used flexure hinge contours and additionally for the rigid-body model. Regarding a consistent modeling, the coordinate system is defined at the fixed support in the following.

The results for the path deviation compared with the rigid-body model confirm the impact of the synthesis approach for the mechanism with different power


Figure 11.

FEM results for the motion behavior of the Roberts mechanisms ($\beta_1 = 1$, $\beta_h = 0.03$): (a) model and deformed state for input $s = u_{xP} = 10$ mm and (b) straight-line deviation of P ; the curves are drawn in dashed lines from the input displacement at which ε_{adm} is exceeded.

function contours regarding a higher path precision (compared to identical corner-filled contours) and the possible required large stroke (compared to identical semicircular and power function contours with $n = 4$). Furthermore, analyzing the straight-line deviation, it becomes obvious that a more precise rectilinear motion can be realized using the compliant mechanism with individually shaped flexure hinges.

4.3 Nonlinear analytical calculation

The analytical modeling of the compliant mechanisms is also based on the nonlinear theory for large deflections of rodlike structures described in Section 3.3. To consider the coupler point P , a branched mechanism has to be modeled, and the rod is split into three sections in K , each with its own rod axis s_1-s_3 (see **Figure 12**). A force-driven analysis is implemented, while the input force is increased until the desired displacement $u_{xP} = 10$ mm is reached. The straight-line deviation, the maximum strain, and the necessary deflection force are determined, too.

From investigations on separate hinges [49] and flexure hinge-based compliant mechanisms [50, 51], it is known that the flexure hinge orientation strongly influences the elasto-kinematic properties of compliant mechanisms. Therefore, a study of the Roberts mechanism is done, while the hinges A_0 and B_0 and A and B are modeled equally mirrored (see **Figure 13**). From the results, the suitable

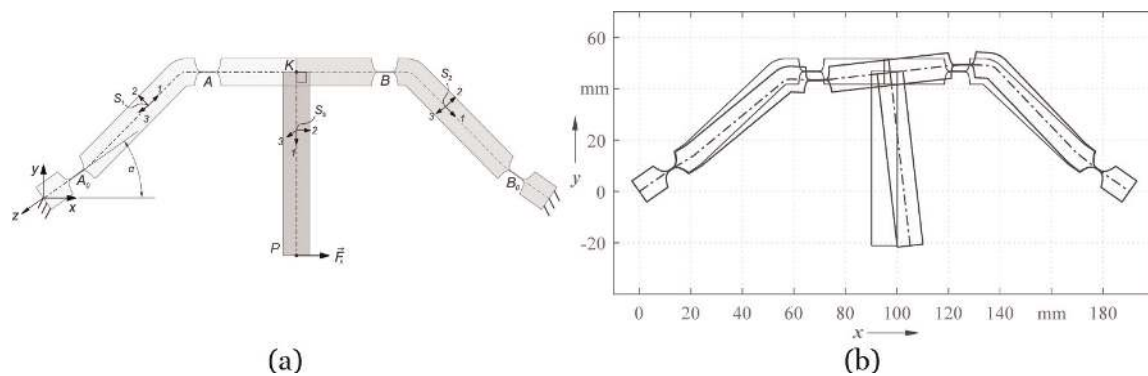


Figure 12. Analytical modeling of the Roberts mechanism ($\beta_1 = 1, \beta_h = 0.03$): (a) branched mechanism with point P split up in three individual rods connected at point K , (b) resulting from MATLAB plot of initial and deflected state for $u_{xP} = 10$ mm ($n_{A_0} = 3, n_A = 12, n_B = 10, n_{B_0} = 3$).

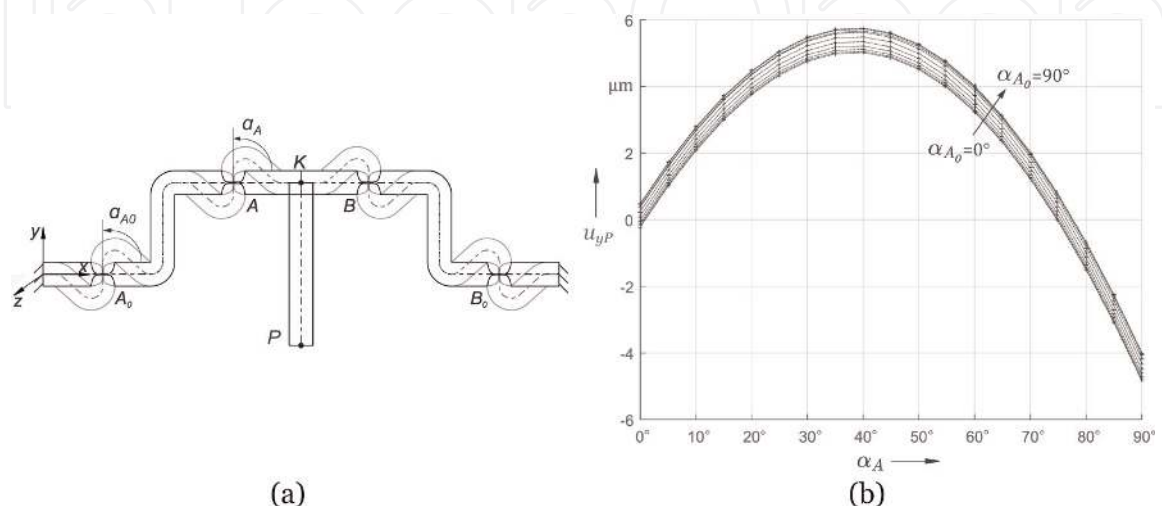


Figure 13. Analytical results for the influence of the flexure hinge orientation on the straight-line deviation of a mechanism with power function contours ($\beta_1 = 1, \beta_h = 0.03, u_{xP} = 10$ mm): (a) model with two variable orientation angles from 0° to 90° and (b) deviation of P .

orientations $\alpha_{A0} = 35^\circ$ and $\alpha_A = 0^\circ$ can be concluded to realize the smallest straight-line deviation.

4.4 Comparison of results

The FEM results and analytical results for the four investigated compliant Roberts mechanisms are in a very good correlation (see **Table 7**).

Generally, all four compliant mechanisms exhibit a very small straight-line deviation in the low micrometer range. With respect to the path deviation compared to rigid-body model, the values differ from the straight-line deviations. However, as for the separate hinge (cf. **Figure 9b**), the mechanism with circular contours provides the smallest path deviation. With regard to the maximum admissible strain, the desired stroke cannot be realized when using identical circular or power function hinges of the fourth order (cf. **Figure 11b**). In contrast, the full stroke is possible when using the corner-filleted hinges and, as expected, also with the synthesized mechanism with individually shaped hinges. Furthermore, the input force varies considerably, and, thus, a required stiffness can be achieved, too.

Hence, the result method independently confirms the practicability and impact of the angle-based synthesis method for different hinges in one mechanism. Moreover, the presented nonlinear analytical approach is suitable to accurately model the elasto-kinematic properties of planar flexure hinge-based compliant mechanisms under consideration of the specific hinge contour without simulations.

4.5 Geometric scaling approach

The influence of the scale on the deformation and motion behavior is a further relevant aspect regarding the similitude of mechanisms [52]. Based on investigations of a separate flexure hinge and a compliant parallel linkage [53], the uniform geometric scaling may also be a suitable synthesis approach for compliant mechanisms if the change ratios of the elasto-kinematic properties are known.

Here, uniform geometric scaling is understood as a linear variation of all geometric length parameters with the scale factor of the value g , while the initial dimension $H = 10$ mm is considered for $g = 1$. The geometric scaling approach is exemplified for the Roberts mechanism with different power function hinges based

Hinge contours	Method	Straight-line deviation u_{yP} [μm]	Path deviation $ u_{yP} - u_{yP}^* $ [μm]	Input force F_x [N]	Maximum strain ϵ_{\max} [%]
Identical circular, $R = H/2$ (Figure 10a)	FEM	-13.20	11.53	4.93	1.84
	Analytical	-13.72	11.02	4.61	1.88
Identical corner-filleted, $r = 0.1l$ (Figure 10b)	FEM	13.20	37.93	0.80	0.36
	Analytical	13.65	38.38	0.78	0.33
Identical power function, $n = 4$ (Figure 10c)	FEM	-8.99	15.74	2.13	0.85
	Analytical	-9.23	15.50	2.16	0.89
Different power function (Figure 10d)	FEM	1.29	26.02	1.30	0.46
	Analytical	0.86	25.59	1.25	0.47

Table 7.

Comparison of FEM and analytical results for the elasto-kinematic properties of the Roberts mechanisms with identical common hinge contours and with different power function contours ($\beta_1 = 1$, $\beta_h = 0.03$, $\beta_w = 0.6$, with $H = 10$ mm and input $u_{xP} = 10$ mm).

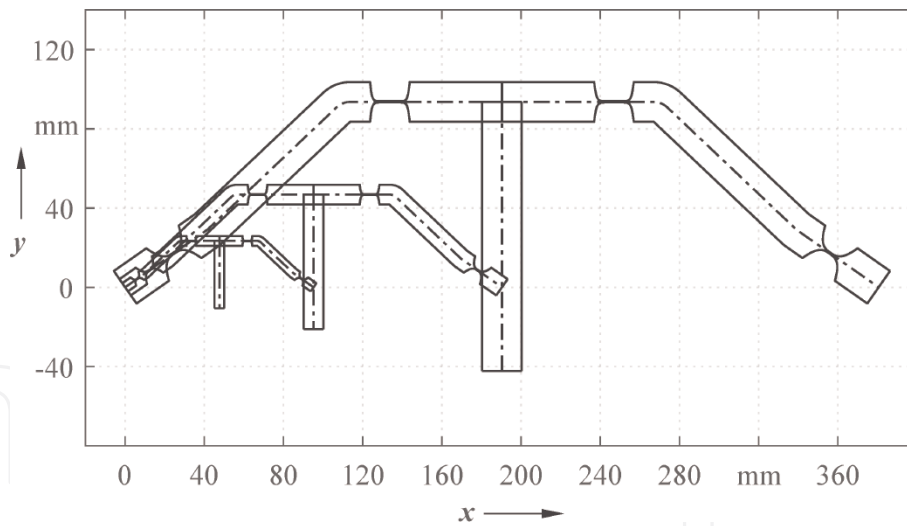


Figure 14. Geometric scaling of the compliant Roberts mechanism shown for the factors $g = 0.5$, $g = 1$, and $g = 2$ (mechanism with different power function hinges, $\beta_1 = 1$, $\beta_h = 0.03$).

Scaling factor	Stroke u_{xP} [mm]	Straight-line deviat. u_{yP}^* [μm]	Straight-line deviat. u_{yP} [μm]	Path deviation $ u_{yP} - u_{yP}^* $ [μm]	Input force F_x [N]	Max. strain ϵ_{max} [%]	Angle φ_A [$^\circ$]
$g = 0.5$	5	-10.78	0.431	11.21	0.123	0.468	10.33
$g = 1$	10	-24.73	0.862	25.59	1.249	0.468	10.33
$g = 2$	20	-49.74	1.725	51.46	4.997	0.468	10.33
$g = 10$	100	-249.91	8.623	258.53	124.930	0.468	10.33

Table 8. Analytical results for the influence of geometric scaling on the elasto-kinematic properties for the mechanism with different power function hinges ($\beta_1 = 1$, $\beta_h = 0.03$, $\beta_w = 0.6$).

on analytical calculations. Therefore, different scaling factors are regarded (see **Figure 14**). The results are mentioned in **Table 8**, while the input stroke u_{xP} is scaled as well.

Based on the results, geometric scaling is an appropriate approach for the accelerated synthesis through the adjustment of an initially designed or used compliant mechanism with known elasto-kinematic properties to each required scale of the new application through the use of the property change ratios concluded in **Table 9**. The ratio is defined as property value for $g \neq 1$ related to property value for $g = 1$. Therefore, performing a new calculation is not necessary anymore. The results are independent of the hinge contour, while a nonuniform scaling is possible, too [53]. Furthermore, this approach can be used to significantly increase the stroke by increasing the mechanism size or to reduce the straight-line deviation by miniaturization because strain values and angles are independent of the scale.

Property	Property change ratio
Maximum strain	1
Angular deflection	1
Input displacement, motion path coordinates, path deviations	g
Input/deflection force	g^2

Table 9. Influence of uniform geometric scaling with the factor g on the change ratios of the elasto-kinematic properties of planar flexure hinge-based compliant mechanisms.

5. Conclusions

Flexure hinge-based compliant mechanisms offer a high-precise and large-stroke guidance motion with straight-line or path deviations in the single-micrometer range if they are purposefully designed. It is shown that the synthesis of a compliant mechanism with individually shaped flexure hinges based on the relative rotation angles in the rigid-body model is a suitable and general synthesis method which is easy to use without the need of numerical calculations, FEM simulations, or a multi-criterial optimization (cf. [25, 35]). Therefore, this chapter provides a survey of several approaches, guidelines, and aids for the accurate and comprehensive design of notch flexure hinges using various hinge contours, while power function contours are particularly suitable. The use of design graphs, design equations, a computational design tool, or a geometric scaling approach is briefly presented. The results are verified by analytical calculations and FEM simulations, and also, not mentioned, by experimental investigations (e.g., [3, 24, 33]). Moreover, especially the used nonlinear analytical approach has a great potential for the future work, for example, the implementation of a GUI for the compliant mechanism synthesis.

Acknowledgements

We acknowledge support for the research by the DFG (Grant no. ZE 714/10-2). We further acknowledge support for the Publishing Process Charge by the Thuringian Ministry for Economic Affairs, Science and Digital Society and the Open Access Publication Fund of the Technische Universität Ilmenau.

Conflict of interest

We declare that we have no conflict of interest.


IntechOpen

Author details

Sebastian Linß*, Stefan Henning and Lena Zentner
Compliant Systems Group, Technische Universität Ilmenau, Ilmenau, Germany

*Address all correspondence to: sebastian.linss@tu-ilmenau.de

IntechOpen

© 2019 The Author(s). Licensee IntechOpen. This chapter is distributed under the terms of the Creative Commons Attribution License (<http://creativecommons.org/licenses/by/3.0>), which permits unrestricted use, distribution, and reproduction in any medium, provided the original work is properly cited. 

References

- [1] Howell LL, Magleby SP, Olsen BM. Handbook of Compliant Mechanisms. Chichester: Wiley; 2013. 324 p
- [2] Zentner L. Nachgiebige Mechanismen. München: De Gruyter Oldenbourg; 2014. 133 p
- [3] Gräser P, Linß S, Harfensteller F, Zentner L, Theska R. Large stroke ultra-precision planar stage based on compliant mechanisms with polynomial flexure hinge design. In: Proceedings of the 17th Euspen; Hannover, Germany. 2017. pp. 207-208
- [4] Teo TJ, Yang G, Chen I-M. A large deflection and high payload flexure-based parallel manipulator for UV nanoimprint lithography: Part I. Modeling and analyses. Precision Engineering. 2014;**38**(4):861-871. DOI: 10.1016/j.precisioneng.2014.05.003
- [5] Beroz J, Awtar S, Bedewy M, Tawfick S, Hart AJ. Compliant microgripper with parallel straight-line jaw trajectory for nanostructure manipulation. In: Proceedings of the 26th Annual Meeting of the ASPE; Denver, USA. 2011
- [6] Darnieder M, Pabst M, Wenig R, Zentner L, Theska R, Fröhlich T. Static behavior of weighing cells. Journal of Sensors and Sensor Systems. 2018;**7**(2): 587-600. DOI: 10.5194/jsss-7-587-2018
- [7] Lobontiu N. Compliant Mechanisms: Design of Flexure Hinges. Boca Raton, Fla: CRC Press; 2003. 447 p
- [8] Pavlovic NT, Pavlovic ND. Compliant mechanism design for realizing of axial link translation. Mechanism and Machine Theory. 2009; **44**(5):1082-1091. DOI: 10.1016/j.mechmachtheory.2008.05.005
- [9] Xu Q. Design and Implementation of Large-Range Compliant Micropositioning Systems. Singapore: John Wiley & Sons Singapore Pte. Ltd; 2016. 273 p
- [10] Henein S, Spanoudakis P, Droz S, Myklebust LI, Onillon E. Flexure pivot for aerospace mechanisms. In: Proceedings of the 10th European Space Mechanisms and Tribology Symposium; San Sebastian, Spain. 2003
- [11] Cosandier F, Eichenberger A, Baumann H, Jeckelmann B, Bonny M, Chatagny V, et al. Development and integration of high straightness flexure guiding mechanisms dedicated to the METAS watt balance mark II. Metrologia. 2014;**51**(2):88-95. DOI: 10.1088/0026-1394/51/2/S88
- [12] Lin C-F, Shih C-J. Multiobjective design optimization of flexure hinges for enhancing the performance of micro-compliant mechanisms. Journal of the Chinese Institute of Engineers. 2005;**28**(6):999-1003. DOI: 10.1080/02533839.2005.9671075
- [13] Linß S, Erbe T, Zentner L. On polynomial flexure hinges for increased deflection and an approach for simplified manufacturing. In: Proceedings of the 13th World Congress in Mechanism and Machine Science; Guanajuato, Mexico. 2011. A11_512
- [14] Henning S, Linß S, Zentner L. detasFLEX—A computational design tool for the analysis of various notch flexure hinges based on non-linear modeling. Mechanical Sciences. 2018;**9**(2):389-404. DOI: 10.5194/ms-9-389-2018
- [15] Howell LL, Midha A. A method for the design of compliant mechanisms with small-length flexural pivots. Journal of Mechanical Design. 1994; **116**(1):280-290. DOI: 10.1115/1.2919359
- [16] Frecker MI, Ananthasuresh GK, Nishiwaki S, Kota S. Topological

- synthesis of compliant mechanisms using multi-criteria optimization. *Journal of Mechanical Design*. 1997; **119**(2):238-245. DOI: 10.1115/1.2826242
- [17] Hopkins JB, Culpepper ML. Synthesis of multi-degree of freedom, parallel flexure system concepts via freedom and constraint topology (FACT)—Part I: Principles. *Precision Engineering*. 2010; **34**(2):259-270. DOI: 10.1016/j.precisioneng.2009.06.008
- [18] Pavlovic ND, Petkovic D, Pavlovic NT. Optimal selection of the compliant mechanism synthesis method. In: *Proceedings of the International Conference Mechanical Engineering in XXI Century*; Niš, Serbia. 2010. pp. 247-250
- [19] Pavlovic NT, Pavlovic ND. Motion characteristics of the compliant four-bar linkages for rectilinear guiding. *Journal of Mechanical Engineering Design*. 2003; **6**(1):20-27
- [20] Hricko J. Straight-line mechanisms as one building element of small precise robotic devices. *Applied Mechanics and Materials*. 2014; **613**:96-101. DOI: 10.4028/www.scientific.net/AMM.613.96
- [21] Wan S, Xu Q. Design and analysis of a new compliant XY micropositioning stage based on Roberts mechanism. *Mechanism and Machine Theory*. 2016; **95**:125-139. DOI: 10.1016/j.mechmachtheory.2015.09.003
- [22] Li J, Chen G. A general approach for generating kinetostatic models for planar flexure-based compliant mechanisms using matrix representation. *Mechanism and Machine Theory*. 2018; **129**:131-147. DOI: 10.1016/j.mechmachtheory.2018.07.015
- [23] Clark L, Shirinzadeh B, Zhong Y, Tian Y, Zhang D. Design and analysis of a compact flexure-based precision pure rotation stage without actuator redundancy. *Mechanism and Machine Theory*. 2016; **105**:129-144. DOI: 10.1016/j.mechmachtheory.2016.06.017
- [24] Linß S. Ein Beitrag zur geometrischen Gestaltung und Optimierung prismatischer Festkörpergelenke in nachgiebigen Koppelmechanismen [doctoral thesis]. Ilmenau: TU Ilmenau; 2015. URN: urn:nbn:de:gbv:ilm1-2015000283
- [25] Linß S, Milojevic A, Pavlovic ND, Zentner L. Synthesis of compliant mechanisms based on goal-oriented design guidelines for prismatic flexure hinges with polynomial contours. In: *Proceedings of the 14th World Congress in Mechanism and Machine Science*; Taipei, Taiwan. 2015. DOI: 10.6567/IFTtoMM.14TH.WC.PS10.008
- [26] Meng Q. A design method for flexure-based compliant mechanisms on the basis of stiffness and stress characteristics [doctoral thesis]. Bologna: Universität Bologna; 2012. DOI: 10.6092/unibo/amsdottorato/4734
- [27] Carbone G, Liang C, Ceccarelli M, Burisch A, Raatz A. Design and simulation of a binary actuated parallel micro-manipulator. In: *Proceedings of the 13th World Congress in Mechanism and Machine Science*; Guanajuato, Mexico. 2011. A12_332
- [28] Wuest W. Blattfedergelenke für Meßgeräte. *Feinwerktechnik*. 1950; **54**(7):167-170
- [29] Jensen BD, Howell LL. The modeling of cross-axis flexural pivots. *Mechanism and Machine Theory*. 2002; **37**(5):461-476. DOI: 10.1016/S0094-114X(02)00007-1
- [30] Bi S, Zhao S, Zhu X. Dimensionless design graphs for three types of annulus-shaped flexure hinges. *Precision Engineering*. 2010; **34**(3):

659-667. DOI: 10.1016/j.precisioneng.2010.01.002

[31] Paros JM, Weisbord L. How to design flexure hinges. *Machine Design*. 1965;25(11):151-156

[32] Zentner L, Linß S. *Compliant Systems – Mechanics of Elastically Deformable Mechanisms, Actuators and Sensors*. München: De Gruyter Oldenbourg; 2019. 166 p

[33] Linß S, Schorr P, Zentner L. General design equations for the rotational stiffness, maximal angular deflection and rotational precision of various notch flexure hinges. *Mechanical Sciences*. 2017;8(1):29-49. DOI: 10.5194/ms-8-29-2017

[34] Zhu BL, Zhang XM, Fatikow S. Design of single-axis flexure hinges using continuum topology optimization method. *Science in China/E*. 2014;57(3):560-567. DOI: 10.1007/s11431-013-5446-4

[35] Gräser P, Linß S, Zentner L, Theska R. Optimization of compliant mechanisms by use of different polynomial flexure hinge contours. In: *Proceedings of the 3rd IAK, Interdisciplinary Applications of Kinematics*; Lima, Peru. 2018. DOI: 10.1007/978-3-030-16423-2_25

[36] Linß S, Erbe T, Theska R, Zentner L. The influence of asymmetric flexure hinges on the axis of rotation. In: *Proceedings of the 56th International Scientific Colloquium*; Ilmenau, Germany. 2011. URN: urn:nbn:de:gbv:ilm1-2011iwk-006:6

[37] Zettl B, Szyszkowski W, Zhang WJ. On systematic errors of two-dimensional finite element modeling of right circular planar flexure hinges. *Journal of Mechanical Design*. 2005;127(4):782-787. DOI: 10.1115/1.1898341

[38] Yong YK, Lu T-F, Handley DC. Review of circular flexure hinge design

equations and derivation of empirical formulations. *Precision Engineering*. 2008;32(2):63-70. DOI: 10.1016/j.precisioneng.2007.05.002

[39] Valentini PP, Pennestrì E. Elasto-kinematic comparison of flexure hinges undergoing large displacement. *Mechanism and Machine Theory*. 2017;110:50-60. DOI: 10.1016/j.mechmachtheory.2016.12.006

[40] Venanzi S, Giesen P, Parenti-Castelli V. A novel technique for position analysis of planar compliant mechanisms. *Mechanism and Machine Theory*. 2005;40(11):1224-1239. DOI: 10.1016/j.mechmachtheory.2005.01.009

[41] Raatz A. *Stoffschlüssige Gelenke aus pseudo-elastischen Formgedächtnislegierungen in Pararellrobotern* [doctoral thesis]. Braunschweig: TU Braunschweig; 2006

[42] Zelenika S, Munteanu MG, De Bona F. Optimized flexural hinge shapes for microsystems and high-precision applications. *Mechanism and Machine Theory*. 2009;44(10):1826-1839. DOI: 10.1016/j.mechmachtheory.2009.03.007

[43] Torres Melgarejo MA, Darnieder M, Linß S, Zentner L, Fröhlich T, Theska R. On Modeling the bending stiffness of thin semi-circular flexure hinges for precision applications. *Actuators*. 2018;7(4):86. DOI: 10.3390/act7040086

[44] Tseytlin YM. Notch flexure hinges: An effective theory. *The Review of Scientific Instruments*. 2002;73(9):3363-3368. DOI: 10.1063/1.1499761

[45] Dirksen F, Lammering R. On mechanical properties of planar flexure hinges of compliant mechanisms. *Mechanical Sciences*. 2011;2:109-117. DOI: 10.5194/ms-2-109-2011

- [46] Campanile LF, Hasse A. A simple and effective solution of the elastica problem. The Proceedings of the Institution of Mechanical Engineers, Part C: Journal of Mechanical Engineering Science. 2008;222(12): 2513-2516. DOI: 10.1243/09544062JMES1244
- [47] Ryu JW, Gweon D-G. Error analysis of a flexure hinge mechanism induced by machining imperfection. Precision Engineering. 1997;21(2/3):83-89. DOI: 10.1016/S0141-6359(97)00059-7
- [48] Linß S, Schorr P, Henning S, Zentner L. Contour-independent design equations for the calculation of the rotational properties of commonly used and polynomial flexure hinges. In: Proceedings of the 59th International Scientific Colloquium; Ilmenau, Germany. 2017. URN: urn:nbn:de:gbv:ilm1-2017iwk-001:5
- [49] Schorr P, Linß S, Zentner L, Zimmermann K. Influence of the orientation of flexure hinges on the elasto-kinematic properties. In: Tagungsband Vierte IFToMM D-A-CH Konferenz 2018; Lausanne, Switzerland. 2018. DOI: 10.17185/dupublico/45330
- [50] Gräser P, Linß S, Zentner L, Theska R. On the influence of the flexure hinge orientation in planar compliant mechanisms for ultra-precision applications. In: Proceedings of the 59th International Scientific Colloquium; Ilmenau, Germany. 2017. URN: urn:nbn:de:gbv:ilm1-2017iwk-090:9
- [51] Hao G, Yu J, Liu Y. Compliance synthesis of a class of planar compliant parallelogram mechanisms using the position space concept. In: Proceedings of the 4th ReMAR Conference; Delft, The Netherlands. 2018. DOI: 10.1109/REMAR.2018.8449882
- [52] Laudahn S, Sviberg M, Wiesenfeld L, Haberl F, Haidl J, Abdul-Sater K, et al. Similitude of scaled and full scale linkages. In: Proceedings of the 7th European Conference on Mechanism Science: EuCoMeS; Aachen, Germany. 2018. pp. 256-264. DOI: 10.1007/978-3-319-98020-1_30
- [53] Linß S, Gräser P, Räder T, Henning S, Theska R, Zentner L. Influence of geometric scaling on the elasto-kinematic properties of flexure hinges and compliant mechanisms. Mechanism and Machine Theory. 2018;125(C): 220-239. DOI: 10.1016/j.mechmachtheory.2018.03.008